

To smooth or not to smooth? ROC analysis of perfusion fMRI data

Jiongjiong Wang^{a,c,*}, Ze Wang^{b,c}, Geoffrey K. Aguirre^{b,c}, John A. Detre^{b,c}

^aDepartment of Radiology, University of Pennsylvania, Philadelphia, PA 19104, USA

^bDepartment of Neurology, University of Pennsylvania, Philadelphia, PA 19104, USA

^cCenter for Functional Neuroimaging, University of Pennsylvania, Philadelphia, PA 19104, USA

Received 3 August 2004; accepted 15 November 2004

Abstract

Blood oxygenation level dependent (BOLD) contrast has been widely used for visualizing regional neural activation. Temporal filtering and parameter estimation algorithms are generally used to account for the intrinsic temporal autocorrelation present in BOLD data. Arterial spin labeling perfusion imaging is an emerging methodology for visualizing regional brain function both at rest and during activation. Perfusion contrast manifests different noise properties compared with BOLD contrast, represented by the even distribution of noise power and spatial coherence across the frequency spectrum. Consequently, different strategies are expected to be employed in the statistical analysis of functional magnetic resonance imaging (fMRI) data based on perfusion contrast. In this study, the effect of different analysis methods upon signal detection efficacy, as assessed by receiver operator characteristic (ROC) measures, was examined for perfusion fMRI data. Simulated foci of neural activity of varying amplitude and spatial extent were added to resting perfusion data, and the accuracy of each analysis was evaluated by comparing the results with the known distribution of pseudo-activation. In contrast to the BOLD fMRI, temporal smoothing or filtering reduces the power of perfusion fMRI data analyses whereas spatial smoothing is beneficial to the efficacy of analyses.

© 2005 Elsevier Inc. All rights reserved.

Keywords: Arterial spin labeling (ASL); Cerebral blood flow (CBF); Receiver operator characteristic (ROC); Spatial smoothing; Temporal smoothing; Functional brain imaging

1. Introduction

Functional magnetic resonance imaging (fMRI) based on the blood oxygenation level dependent (BOLD) contrast has become a standard method for visualizing regional neural activation. A consensus has emerged that valid statistical inference, hence plausible interpretation of the neuronal mechanism, can only be achieved by meticulous choice of appropriate data analysis methods in BOLD fMRI. This concern regarding the validity of neuroimaging studies using fMRI arises mainly due to a robust observation that BOLD image series possess temporal autocorrelation or “smoothness,” manifested as elevated power in the lower frequency range of the power spectrum accompanied by less dominating broad-band components [1–5]. Various approaches have been introduced to accommodate serial correlation in the context of parameter estimation with general linear model (GLM). A general dichotomy of these

methods has been proposed by Friston et al. [6], which includes (1) “whitening” of the time series with an exquisite understanding of the noise characteristics [7,8] and (2) “smoothing” (“filtering”) of the time series to impose a known correlation structure [9]. It has been proposed that band-pass filtering, and implicitly smoothing, provides an optimal solution to minimize bias while maintaining a reasonable degree of efficiency in BOLD fMRI.

Arterial spin labeling (ASL) perfusion imaging is an emerging and alternative methodology for functional neuroimaging studies [10,11]. In contrast to BOLD fMRI that relies on the susceptibility effects in and around the venous vasculature [12], ASL perfusion contrast is based on alternations in the longitudinal relaxation of brain tissue caused by changes in regional blood flow [13]. Consequently, perfusion contrast may yield more specific functional localization [14,15] and reduced sensitivity to static susceptibility effects [16], although the size of signal changes induced by task activation is generally smaller in ASL than BOLD fMRI. Because perfusion image series are generated by pair-wise subtraction of temporally adjacent

* Corresponding author. Tel.: +1 215 614 0631; fax: +1 215 349 8260.
E-mail address: jwang3@mail.med.upenn.edu (J. Wang).

control and label acquisitions, the noise properties of ASL perfusion contrast are also distinctive from those of the BOLD contrast. Recent studies demonstrate that perfusion data manifest relatively even distribution of noise power across the frequency spectrum [17,18], i.e., image time series acquired using ASL possess minimal correlation in time. This natural “white-noise” property predicts that perfusion time series without any temporal manipulation (“filtering” or “smoothing”) should provide the most efficient parameter estimation in statistical analyses [6]. The accuracy and validity of the statistical inference using such a conventional GLM analysis was recently demonstrated by assessing the false-positive rates in null-hypothesis perfusion fMRI data [17]. Despite the evidence for a flat noise distribution, temporal autocorrelation may still be present in perfusion fMRI data, but buried in the relatively large noise, therefore not observed in the mean power spectrum averaged across voxels. The experimental support for such speculation is that the perfusion-based hemodynamic function follows a very close temporal evolution as that observed in BOLD fMRI [19,20]. Temporal smoothing, particularly a “matched filter,” is therefore beneficial for detecting small signal out of a white-noise background based on prior knowledge of the target signal [21]. The prime aim of the present work is to address the question whether perfusion data should be temporally smoothed or not smoothed for efficient and accurate parameter estimation.

Besides temporal smoothing, spatial smoothing has become a routine step in the analysis of fMRI data, to improve signal detection as well as to better characterize (stabilize) the spatial smoothness [22,23]. In BOLD fMRI, it has been found that signal components with lower temporal frequencies tend to be more coherent across space than components with higher temporal frequency [1,17,24]. As a consequence, spatial smoothing of BOLD data acts to augment temporal noise in the low-frequency range and can deleteriously impact experimental power. Perfusion fMRI data, in contrast, seem not to show a dependence on the temporal frequency with respect to its degree of spatial coherence [17]. Spatial smoothing is therefore expected to improve the sensitivity of perfusion fMRI without exacerbating the confounding effect due to slow baseline drifts. The second question to be addressed in this paper is whether and to what extent spatial smoothing should be carried out in perfusion fMRI to yield accurate signal detection and appropriate statistics.

To these ends, the receiver operator characteristic (ROC) method [25] was employed to assess the performance and efficacy of various data analysis approaches in perfusion fMRI, especially the effects of temporal and spatial smoothing. The ROC method has been previously used as a tool for objective comparisons of various strategies in BOLD fMRI [26,27]. Its advantage is that the methodological performance can be compared without referring to the statistical significance of the result, which is still difficult to define and may vary for each analysis. In the

present work, we generated data sets by introducing simulated activation foci with known intensity and spatial extent into fMRI data acquired during resting states. The accuracy of each analysis was evaluated according to its ability to detect most of the “real” activations while minimizing the detection of “false” activations.

2. Methods

2.1. MR scanning

MR scanning was carried out on a 1.5-T whole-body system (GE Medical Systems, Milwaukee, WI), with the product quadrature head coil. Written informed consent was obtained prior to all human studies according to an Institutional Review Board approval. Perfusion imaging was performed on 10 healthy subjects (19–27 years, 5 female, mean 24.1 years) using a pulsed ASL (PASL) method, as described previously [17,28]. The PASL sequence was a modified version of the flow-sensitive alternating inversion recovery (FAIR) [29] technique, in which a saturation pulse was applied at 800 ms after the inversion pulse [frequency offset corrected inversion (FOCI), 16 ms, BW 10 kg] [30], similar to QUIPSS II (Quantitative Imaging of Perfusion using a Single Subtraction) [31]. A gradient-echo echo-planar imaging (EPI) sequence was used for image acquisition, and the parameters were FOV=24×16 cm, 64×40 matrix, TR/TE=3000/18 ms, bandwidth 100 kHz, flip angle=90°, slice thickness 8 mm, interslice space 2 mm. Eight slices of brain cortex were acquired from inferior to superior in an interleaved order, and each slice acquisition took about 50 ms. Eight minutes of resting state perfusion scan (160 acquisitions) was carried out on each subject while the subject was instructed to relax with eyes open. A 30-s two-point T1 measurement sequence was carried out after the scan for cerebral blood flow (CBF) quantification. Nine of the 10 subjects also underwent BOLD fMRI scans using a gradient-echo EPI sequence which was the same as that used in PASL scans, and the parameters were FOV=24×16 cm, 64×40 matrix, TR/TE=2000/50 ms, bandwidth 100 kHz, flip angle=90°. Twenty contiguous slices with a thickness of 5 mm were acquired from inferior to superior in an interleaved order. Eight minutes of resting state BOLD data (240 acquisitions) were acquired from these nine subjects. For comparison of the BOLD and perfusion contrast, we only used these nine subjects’ data in the following analyses. The perfusion data were also used in our prior study for testing the false-positive rate under null-hypothesis conditions [17].

2.2. Simulated activation

In each subject, both the BOLD and raw PASL image series were corrected for motion [32]. The series of label images in the PASL scan were shifted in time by one TR using sinc interpolation [18], and the perfusion weighted

image series were generated by pair-wise subtraction between time-matched label and control images. Absolute CBF image series (with 80 samples in each subject) were calculated from the perfusion-weighted image series following the PASL model by incorporating the M_0 maps acquired using the T1 measurement sequence, as described previously [17,33].

Activation time series were added to approximately 5% of the total brain pixels in the motion-corrected BOLD and CBF image series, respectively. The region-of-interest (ROI) of the gray matter was segmented using the SPM99 software package in each subject, which was then used to constrain these activation foci within gray matter regions. This is physiologically reasonable as neuronal activations are generally associated with the brain cortex. For the BOLD data, signal time series in odd and even slices were pair-wise summated (slice resolution down-sampled by a factor of 2) to form a new dataset with 10 slices of 10 mm thickness, so that the BOLD and CBF data had similar spatial resolution for comparison. Because of the increased signal-to-noise ratio (SNR), BOLD data with summated slices yielded about 2% increase in the ROC score compared to the original dataset, but did not affect the results reported in this paper. Three cluster sizes of activation foci were tested, i.e., single voxel ($1 \times 1 \times 1$), 4 contiguous voxels ($2 \times 2 \times 1$) and 32 contiguous voxels ($4 \times 4 \times 2$) with a corresponding volume of 0.14, 0.56 and 4.5 cm^3 , respectively. Hereafter, these three conditions are referred to as the cluster size of 1, 2 and 4 pixels, respectively, according to the in-plane diameter of the given activation foci. These three activation cluster sizes were

tested separately for each of the analysis model in the BOLD and CBF data. For BOLD data, the signal change between the resting and activation states was assumed to be 1.5% of the mean original signal intensity in the corresponding voxel. For perfusion data, three levels of percentage signal change during activation states (25%, 50% and 75% on top of the baseline CBF value) were tested. The ranges of the fractional signal change in BOLD and perfusion data were in line with reported values in sensorimotor and cognitive studies [34]. The added time series was the convolution of a boxcar function and the hemodynamic response function (HRF) in both BOLD and perfusion data. Other shapes of rest/activation function, such as sinusoid, have been tested which yielded similar results as the boxcar function. The HRF in BOLD data was derived from a previous study [35]. The same HRF was used for perfusion data since the shapes of the perfusion and BOLD HRFs are very similar [18–20]. Fig. 1 displays the assumed HRFs along with the representative mean time courses averaged across the activated voxels in both the BOLD and perfusion data. Because the effective temporal resolution was 6 s per sample (2TR), the perfusion HRF manifested minimal smoothness and the overall effect through convolution with the boxcar function was a time delay of about 6 s. The task design was assumed to be 30 s OFF/ON for both the BOLD and CBF image series in each subject.

2.3. Data analysis

BOLD and CBF datasets with assumed activation foci were spatially smoothed with three sizes of Gaussian

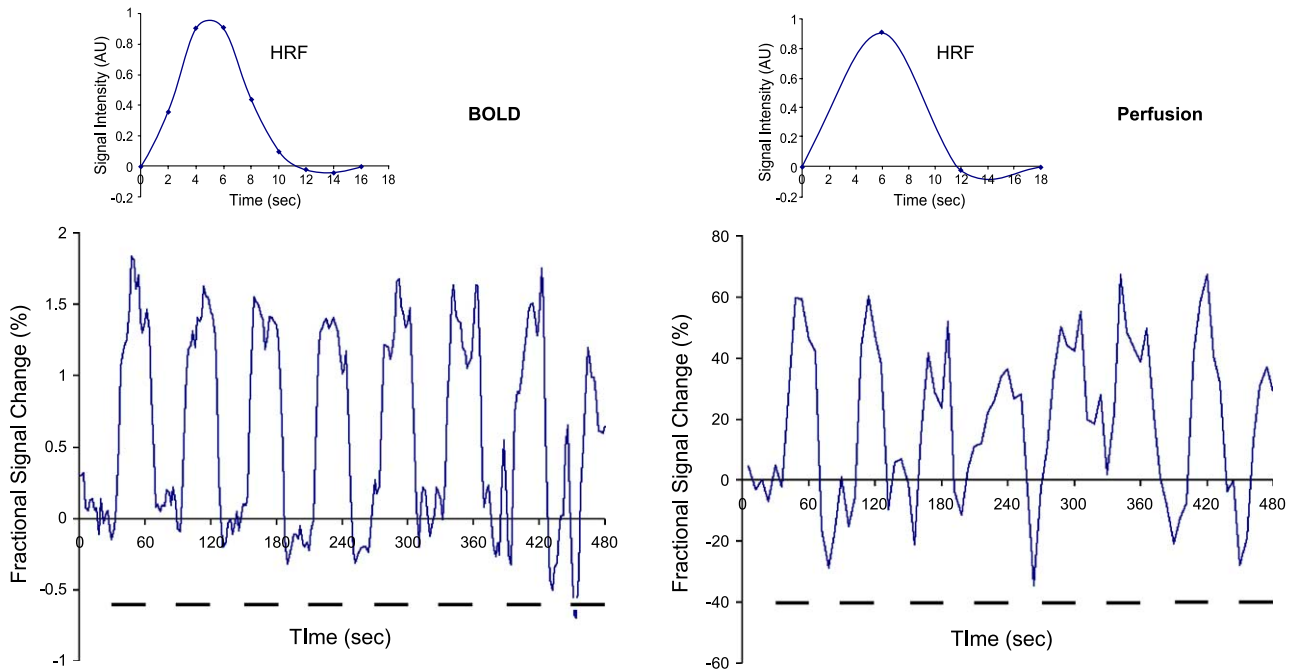


Fig. 1. Assumed hemodynamic response functions (HRF) in the data analysis of perfusion and BOLD fMRI. Also displayed are the mean time courses of the perfusion and BOLD series averaged across the voxels with added activation in a representative subject. The signal change between the resting and activation states is 1.5% and 50% in the BOLD and perfusion data, respectively.

kernel, namely, a full width at half maximum (FWHM) of 1 ($1 \times 1 \times 1$), 2 ($2 \times 2 \times 1$) and 4 ($4 \times 4 \times 2$) in-plane pixels, respectively (the same size as the assumed activation foci). Statistical analyses were carried out using the VoxBo software package (<http://www.VoxBo.org>). The analysis of the BOLD image series followed the modified general linear model [9]. A t -statistic was used to evaluate the significance of the variance in the data explained by the model. The reference function was convolved with the BOLD HRF to account for the temporal delay and smoothness due to hemodynamic effects. To accommodate temporal autocorrelation of the BOLD data, a $1/f$ function was fit to the (square root of the) average BOLD power spectrum, ignoring those frequencies at which power attributable to task might be expected. The time-domain representation of the $1/f$ curve was placed within the \mathbf{K} matrix (the convolution matrix representing all assumed temporal autocorrelation) [1,9] along with a filter designed to remove the low-frequency confounds and high-frequency noise at the Nyquist frequency, and a low-pass kernel representing the standard hemodynamic function [35]. The low-frequency noise to be filtered out was defined as the frequency range containing less than 1% of the power of the frequency spectrum of the reference function.

For perfusion data, the benchmark analysis consisted only of a conventional GLM analysis without temporal smoothing or filtering. Various preprocessing interventions were then assessed, including low-pass, high-pass filtering, temporal smoothing as well as their combinations. As aforementioned, the cutoff of the low- and high-pass filters was determined to avoid power overlap with the presumed reference function. For example, the cutoff of low-frequency noise was generally 2 frequency units (which is the resolution of frequency spectrum) below the main frequency of the task function, while the cutoff of high-frequency components was above the third harmonic of the main task frequency. The attempted temporal smoothing included convolution with HRF (see Fig. 1), moving average of three samples and Gaussian smoothing kernel with a FWHM of two samples. These smoothing kernels were chosen because their temporal scales are similar to that of the perfusion-based HRF. It is worth noting that the temporal smoothness and hence the effective degree of freedom should change when the perfusion image series were smoothed or/and filtered. The time-domain representation of these filters and smooth kernels was placed within the \mathbf{K} matrix for the GLM analysis. A t -test was used to evaluate the significance of the variance in the data explained by the model. The reference function was convolved with the perfusion HRF to account for the temporal delay and potential smoothness.

In order to generate the ROC curves, the brain voxels were ranked from high T scores to low T scores. ROC curves were plotted based on the ratio of true activations vs. false-positive findings throughout the range of ranked T

scores, by comparing with the spatial locations of added activation (see Fig. 2). A single parameter (area under curve, AUC) was used as the surrogate score for the efficacy of each method. An earlier study employed other measure for ROC analysis, such as the mean of the ROC value over a limited range of false-positive ratio between 0 and 0.1 [26]. We also obtained this value in the data analysis which did not show different result compared to the AUC measures and therefore was not reported here. The ROC results were entered into repeated-measures ANOVA using the SPSS software package, to assess the effects of spatial smoothing, activation cluster size, activation intensity and contrast (BOLD and perfusion).

3. Results

3.1. Activation intensity

Fig. 3 displays the mean ROC scores (AUC) as a function of the fractional signal change in perfusion fMRI. The data are spatially smoothed with an intermediate Gaussian kernel of 2-pixel FWHM followed by the benchmark GLM analysis. As expected, the power of perfusion fMRI increases with higher fractional signal change and the main effect is statistically significant by repeated measures ANOVA test ($F(2, 7)=492.0, P<.001$). This effect of activation intensity is quite robust and can be repeated in datasets with different sizes of activation foci (see Fig. 3). Since this result provides a general reference frame for the relationship between the methodological performance and effect size, we use a typical

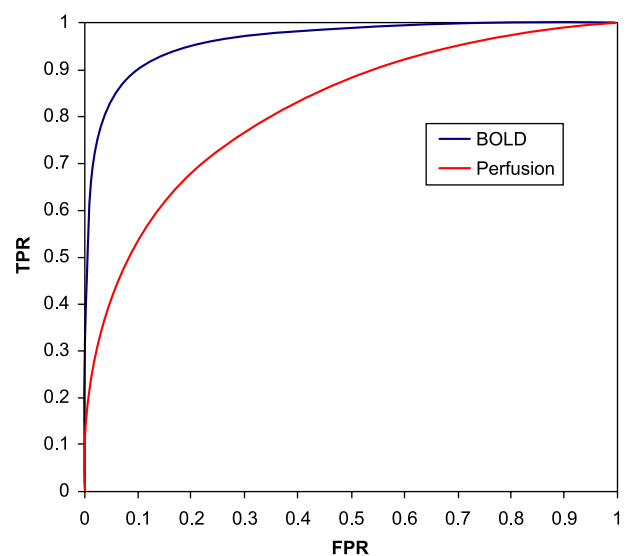


Fig. 2. ROC curves of perfusion and BOLD fMRI obtained from a representative subject at the task frequencies of 30 s OFF/ON. The activation cluster size is 2 pixels in both the perfusion and BOLD data which have been spatially smoothed with a 2-pixel FWHM Gaussian kernel. The benchmark GLM analysis is employed for perfusion fMRI while the BOLD data are analyzed following the modified GLM method. TPR indicates true-positive rate and FPR indicates false-positive rate.

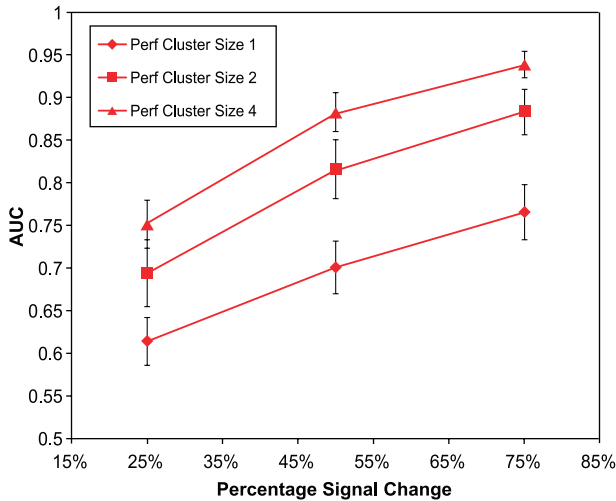


Fig. 3. Mean ROC scores (AUC) of perfusion fMRI as a function of the assumed fractional signal change measured at different activation cluster sizes. The data are spatially smoothed with a 2-pixel FWHM Gaussian kernel and analyzed using the benchmark GLM. The error bars indicate the standard deviation across the nine subjects.

signal change of 50% for perfusion activation in the following analyses.

3.2. Temporal smoothing/filtering

Table 1 lists the mean ROC scores obtained under various conditions of temporal smoothing and filtering in perfusion fMRI. An intermediate spatial smoothing kernel of 2-pixel FWHM is applied in this analysis. Filtering or smoothing of the perfusion image series degrades the accuracy of perfusion fMRI for the design frequency of 30 s OFF/ON, and the effect is statistically significant in all the tested temporal smoothing and filtering methods. We also repeated the above exam for the design frequency of 4 min OFF/ON, and the results are identical. The topic of the effect of temporal smoothing on BOLD fMRI has

Table 1
Mean ROC scores of perfusion fMRI with various temporal smoothing/filtering methods for 30 s OFF/ON task paradigm

Analysis methods	Activation cluster size		
	1 pixel	2 pixels	4 pixels
Benchmark GLM	0.700±0.031	0.816±0.035	0.882±0.023
High-pass filtering*	0.679±0.026	0.788±0.033	0.845±0.036
Low-pass filtering*	0.696±0.034	0.810±0.037	0.877±0.022
Band-pass filtering*	0.670±0.026	0.775±0.036	0.832±0.033
HRF convolution*	0.661±0.021	0.772±0.038	0.848±0.022
Moving average smoothing (3 points)*	0.681±0.032	0.796±0.034	0.869±0.021
Gaussian smoothing (FWHM 2 points)*	0.658±0.021	0.777±0.029	0.850±0.016

* Significant difference between mean ROC scores obtained using the corresponding temporal smoothing/filtering method and the benchmark GLM analysis (repeated measures ANOVA, $P < .05$).

been studied extensively [6,9,26] and therefore is not repeated here.

3.3. Spatial smoothing

The effect of spatial smoothing on the performance of data analysis is assessed by applying different sizes of smoothing kernels on both the BOLD and perfusion data with added activation foci. The benchmark GLM is employed for the statistical analysis of perfusion data. As shown in Fig. 4, the accuracies of BOLD and perfusion fMRI are not affected by the activation cluster size when little spatial smoothing is applied (FWHM of 1 pixel). With heavier spatial smoothing (FWHM >2 pixels), the accuracies of BOLD and perfusion fMRI improve with larger activation cluster size. The interaction of spatial smoothing and activation cluster size is highly significant ($F(4, 5)=306.1, P < .001$), indicating that spatial smoothing enhances spatially focalized signal while suppresses spatially uncorrelated noise. Fig. 4 also indicates that the effect of spatial smoothing is different in BOLD and perfusion fMRI. In perfusion data, the peak ROC score is reached when the activation cluster size and smoothing kernel are similar. In BOLD data, however, the power generally decreases with heavier spatial smoothing or reaches its peak at a smaller smoothing kernel size as compared to the corresponding perfusion data (e.g., BOLD data with an activation cluster size of 4 pixels). The above observation is confirmed by a significant effect of spatial smoothing×contrast interaction ($F(2, 7)=33.5, P < .001$). In general, the performance and accuracy of the perfusion contrast are inferior to BOLD at the tested design frequency of 30 s OFF/ON ($F(1, 8)=103.4, P < .001$). However, the discrepancy between BOLD and perfusion contrasts diminishes with heavier spatial smoothing regardless of the cluster size

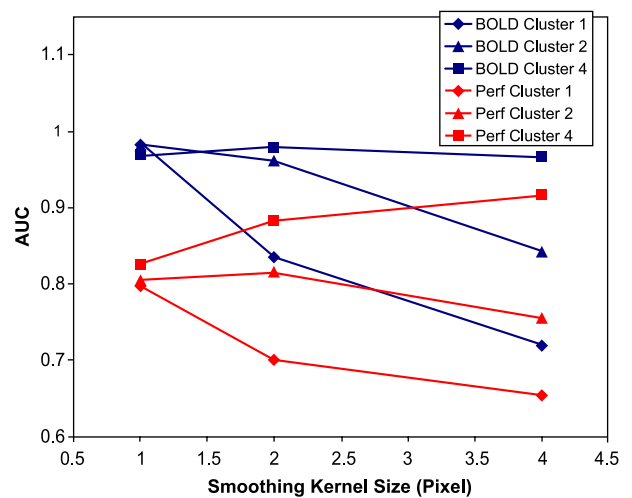


Fig. 4. Mean ROC scores (AUC) of perfusion and BOLD fMRI obtained with different activation cluster sizes and various levels of spatial smoothing. The benchmark GLM and modified GLM are employed for the statistical analysis of perfusion and BOLD data, respectively. The modified GLM is described in the first paragraph of the Data analysis section.

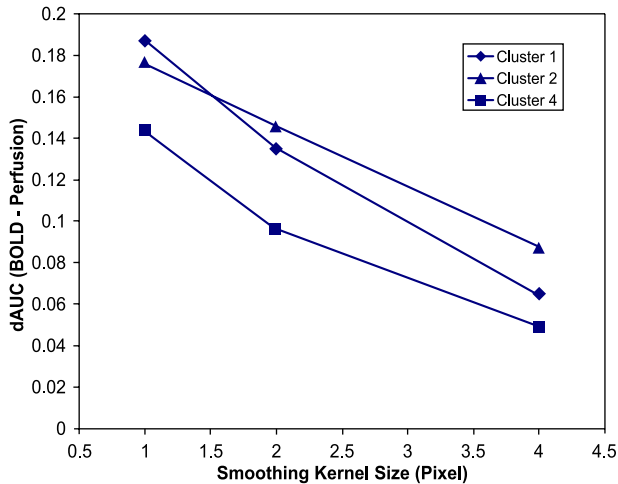


Fig. 5. Mean difference ROC scores (dAUC) between BOLD and perfusion fMRI as a function of the size of the spatial smoothing kernel. The experimental conditions are the same as those shown in Fig. 4. Note the performances of perfusion and BOLD fMRI converges with heavier spatial smoothing.

of activation foci (see Fig. 5), suggesting a beneficial role of spatial smoothing in the statistical analysis of perfusion fMRI.

4. Discussion

Our results of ROC analyses suggest that spatial smoothing generally benefits while temporal smoothing or filtering impairs the efficacy of perfusion fMRI. Following appropriate statistical analysis steps, the performance of perfusion fMRI may approach that of BOLD fMRI, albeit a much lower temporal resolution in perfusion as compared to BOLD data. Previous studies have consistently found that high-pass filtering improves the accuracy of BOLD fMRI by minimizing the low-frequency noise [6,9,26]. Low-pass filtering (temporal smoothing), although having the side effect of enhancing low-frequency noise, benefits the overall performance of BOLD fMRI by reducing the bias through an explicitly imposed noise structure [6]. The general consensus in the data analysis of BOLD fMRI is to achieve an optimal balance of efficiency and accuracy through band-pass filtering and temporal smoothing. In contrast, our results indicate that such temporal manipulation degrades the performance of perfusion fMRI. Conventional signal processing approaches and estimation theory dictate that whitening the data offers the most efficient parameter estimation [36]. Our data are in line with the theoretical prediction since perfusion image series possess an even distribution of power across the frequency spectrum. Introducing temporal filtering or smoothing reduces the effective degree of freedom in the GLM analysis, thereby the efficiencies of perfusion fMRI. The accuracy of parameter estimation is also affected by temporal smoothing or filtering, probably because the effect

of random variation within the preserved frequency range is relatively magnified while other frequency bands are suppressed. One argument against our observation is that serial correlation due to hemodynamic effects may be minimal because our perfusion data were acquired at a low sample rate (6 s per image). We have recently acquired perfusion data with higher sample rate at 3.0 T (TR=2 s, 4 s per perfusion image). Preliminary analyses do not reveal temporal autocorrelation in these datasets, and applying various smoothing kernels repeatedly reduces the ROC score. An earlier study also explored the power spectrum of perfusion data acquired with TR=2 s, but failed to detect any serial correlation in the temporal image series [18]. Future studies may be needed to explore the noise characteristics of perfusion data acquired with high temporal resolution which is becoming feasible recently [37].

Spatial smoothing plays contrasting roles in the data analysis of perfusion and BOLD fMRI. According to image processing theory, spatial smoothing normally improves the SNR and the maximum signal detection occurs when the size of the smoothing kernel approaches the spatial extent of the target signal [36]. Our data on the effect of spatial smoothing on the performance of perfusion fMRI (see Fig. 4) match well with the above theory. In BOLD fMRI, while spatial smoothing is a necessary step to improve SNR and stabilize spatial smoothness [22,23], it can also deleteriously impact the experimental power through augmentation of the low-frequency noise [17,24]. This is because spatially coherent noise in BOLD fMRI has been found to vary systematically across temporal frequencies, in that lower temporal frequencies tend to share phase to a greater extent across space than high frequencies [1]. As a consequence of the magnified confounding effects due to low-frequency noise, BOLD fMRI shows a general trend of reduced detection specificity and decreasing efficacy with heavier spatial smoothing (see Fig. 4). The spatially coherent noise in perfusion data, in contrast, has been demonstrated to follow an even distribution across temporal frequencies [17]. Spatially smoothed perfusion data are therefore not susceptible to slow drift effects, and the result is the convergence (or even crossover) in the efficacies of perfusion and BOLD fMRI with heavier spatial smoothing (see Fig. 5).

5. Conclusion

Using ROC analysis, we provide a reference for appropriate data analysis steps in perfusion fMRI. Our results also confirm previous finding that perfusion fMRI data possess even noise distribution in the power spectrum and spatial coherence.

Acknowledgment

This research was supported by NIH grants HD39621, P41-RR02395, DA015149, NS045839 and NSF grant BCS0224007.

References

- [1] Zarahn E, Aguirre GK, D'Esposito M. Empirical analyses of BOLD fMRI statistics: I. Spatially unsmoothed data collected under null-hypothesis conditions. *Neuroimage* 1997;5(3):179–97.
- [2] Smith AM, Lewis BK, Ruttimann UE, Ye FQ, Sinnwell TM, Yang Y, et al. Investigation of low frequency drift in fMRI signal. *Neuroimage* 1999;9(5):526–33.
- [3] Hyde JS, Biswal BB, Jesmanowicz A. High-resolution fMRI using multislice partial k -space GR-EPI with cubic voxels. *Magn Reson Med* 2001;46(1):114–25.
- [4] Friston KJ, Jezzard P, Turner R. Analysis of functional MRI time-series. *Hum Brain Mapp* 1994;1:153–74.
- [5] Weisskoff RM, Baker J, Belliveau JW, Davis TL, Kwong KK, Cohen MS, et al. Power spectrum analysis of functionally-weighted MR data: what's in the noise? *Proc Int Soc Magn Reson Med* 1993;1:7.
- [6] Friston KJ, Josephs O, Zarahn E, Holmes AP, Rouquette S, Poline J. To smooth or not to smooth? *Neuroimage* 2000;12(2):196–208.
- [7] Bullmore E, Brammer M, Williams SC, Rabe-Hesketh S, Janot N, David A, et al. Statistical methods of estimation and inference for functional MR image analysis. *Magn Reson Med* 1996;35(2):261–77.
- [8] Woolrich MW, Ripley BD, Brady M, Smith SM. Temporal autocorrelation in univariate linear modeling of FMRI data. *Neuroimage* 2001;14(6):1370–86.
- [9] Worsley KJ, Friston KJ. Analysis of fMRI time-series revisited — again. *Neuroimage* 1995;2:173–82.
- [10] Detre JA, Alsop DC. Perfusion fMRI with arterial spin labeling (ASL). In: Moonen CTW, Bandettini PA, editors. *Functional MRI*. Heidelberg: Springer; 1999. p. 47–62.
- [11] Wong EC. Potential and pitfalls of arterial spin labeling based perfusion imaging techniques for MRI. In: Moonen CTW, Bandettini PA, editors. *Functional MRI*. Heidelberg: Springer; 1999. p. 63–9.
- [12] Hoogenraad FG, Pouwels PJ, Hofman MB, Reichenbach JR, Sprenger M, Haacke EM. Quantitative differentiation between BOLD models in fMRI. *Magn Reson Med* 2001;45(2):233–46.
- [13] Detre JA, Wang J. Technical aspects and utilities of fMRI using BOLD and ASL. *Clin Neurophysiol* 2002;113:621–34.
- [14] Duong TQ, Kim DK, Ugurbil K, Kim SG. Localized cerebral blood flow response at submillimeter columnar resolution. *Proc Natl Acad Sci U S A* 2001;98:10904–9.
- [15] Luh WM, Wong EC, Bandettini PA, Ward BD, Hyde JS. Comparison of simultaneously measured perfusion and BOLD signal increases during brain activation with T(1)-based tissue identification. *Magn Reson Med* 2000;44(1):137–43.
- [16] Wang J, Li L, Roc AC, Alsop DC, Tang K, Butler N, et al. Reduced susceptibility effect in perfusion fMRI using single-shot spin-echo EPI acquisitions. *Magn Reson Imaging* 2004;22(1):1–7.
- [17] Wang J, Aguirre GK, Kimberg DY, Detre JA. Empirical analyses of null-hypothesis perfusion fMRI data at 1.5 and 4T. *Neuroimage* 2003;19(4):1449–62.
- [18] Aguirre GK, Detre JA, Zarahn E, Alsop DC. Experimental design and the relative sensitivity of BOLD and perfusion fMRI. *Neuroimage* 2002;15(3):488–500.
- [19] Yang Y, Engelen W, Pan H, Xu S, Silbersweig DA, Stern E. A CBF-based event-related brain activation paradigm: characterization of impulse-response function and comparison to BOLD. *Neuroimage* 2000;12(3):287–97.
- [20] Liu HL, Pu Y, Nickerson LD, Liu Y, Fox PT, Gao JH. Comparison of the temporal response in perfusion and BOLD-based event-related functional MRI. *Magn Reson Med* 2000;43(5):768–72.
- [21] Frackowiak RSJ, Friston K, Frith C, Dolan R, Mazziotta J. *Human brain function*. San Diego: Academic Press; 1997.
- [22] Worsley KJ, Evans AC, Marrett S, Neelin P. A three-dimensional statistical analysis for CBF activation studies in human brain. *J Cereb Blood Flow Metab* 1992;12(6):900–18.
- [23] Poline JB, Mazoyer BM. Enhanced detection in brain activation maps using a multifiltering approach. *J Cereb Blood Flow Metab* 1994;14(4):639–42.
- [24] Aguirre GK, Zarahn E, D'Esposito M. Empirical analyses of BOLD fMRI statistics: II. Spatially smoothed data collected under null-hypothesis and experimental conditions. *Neuroimage* 1997;5(3):199–212.
- [25] Metz CE. Basic principle of ROC analysis. *Semin Nucl Med* 1978;VIII(4):283–98.
- [26] Skudlarski P, Constable RT, Gore JC. ROC analysis of statistical methods used in functional MRI: individual subjects. *Neuroimage* 1999;9:311–29.
- [27] Constable RT, Skudlarski P, Gore JC. An ROC approach for evaluating functional brain MR imaging and postprocessing protocols. *Magn Reson Med* 1995;34(1):57–64.
- [28] Wang J, Alsop DC, Li L, Listerud J, Gonzalez-At JB, Schnall MD, et al. Comparison of quantitative perfusion imaging using arterial spin labeling at 1.5 and 4.0 Tesla. *Magn Reson Med* 2002;48(2):242–54.
- [29] Kim SG. Quantification of relative cerebral blood flow change by flow-sensitive alternating inversion recovery (FAIR) technique: application to functional mapping. *Magn Reson Med* 1995;34:293–301.
- [30] Yongbi MN, Yang Y, Frank JA, Duyn JH. Multislice perfusion imaging in human brain using the C-FOCI inversion pulse: comparison with hyperbolic secant. *Magn Reson Med* 1999;42(6):1098–105.
- [31] Wong EC, Buxton RB, Frank LR. Quantitative imaging of perfusion using a single subtraction (QUIPSS and QUIPSS II). *Magn Reson Med* 1998;39(5):702–8.
- [32] Friston KJ, Ashburner J, Frith CD, Poline JB, Heather JD. Spatial registration and normalization of images. *Hum Brain Mapp* 1995;3:165–89.
- [33] Wang J, Aguirre GK, Kimberg DY, Roc AC, Li L, Detre JA. Arterial spin labeling perfusion fMRI with very low task frequency. *Magn Reson Med* 2003;49(5):796–802.
- [34] Wong EC, Buxton RB, Frank LR. Implementation of quantitative perfusion imaging techniques for functional brain mapping using pulsed arterial spin labeling. *NMR Biomed* 1997;10(4–5):237–49.
- [35] Aguirre GK, Zarahn E, D'Esposito M. The variability of human BOLD hemodynamic responses. *Neuroimage* 1998;8:360–9.
- [36] Ludeman LC. *Random processes: filtering, estimation, and detection*. Hoboken (NJ): John Wiley & Sons; 2002.
- [37] Wong EC, Luh WM, Liu TT. Turbo ASL: arterial spin labeling with higher SNR and temporal resolution. *Magn Reson Med* 2000;44(4):511–5.